The pre-transmembrane region of the human immunodeficiency virus type-1 glycoprotein: a novel fusogenic sequence

Tatiana Suárez[a], Shlomo Nir[b], Félix M. Goñi[a], Asier Saéz-Cirión[a], José L. Nieva[a,*]

[a] *Unidad de Biofísica (CSIC-UPV/EHU) and Departamento de Bioquímica, Universidad del País Vasco, Aptdo. 644, 48080 Bilbao, Spain*
[b] *Seagram Center for Soil and Water Sciences, Faculty of Agricultural, Food and Environmental Quality Sciences, The Hebrew University of Jerusalem, Rehovot 76100, Israel*

Received 20 June 2000

Edited by Hans-Dieter Klenk

Abstract We have investigated membrane interactions and perturbations induced by NH_2-DKWASLWNWFNITNWLWYIK-COOH (HIV_c), representing the membrane interface-partitioning region that precedes the transmembrane anchor of the human immunodeficiency virus type-1 gp41 fusion protein. The HIV_c peptide bound with high affinity to electrically neutral vesicles composed of dioleoylphosphatidylcholine, dioleoylphosphatidylethanolamine and cholesterol (molar ratio, 1:1:1), and induced vesicle leakage and lipid mixing. Infrared spectra suggest that these effects were promoted by membrane-associated peptides adopting an α-helical conformation. A sequence representing a defective gp41 phenotype unable to mediate both cell–cell fusion and virus entry, was equally unable to induce vesicle fusion, and adopted a non-helical conformation in the membrane. We conclude that membrane perturbation and adoption of the α-helical conformation by this gp41 region might be functionally meaningful.

Key words: Membrane fusion; Viral fusion; HIV-1; gp41; Fusion peptide; Peptide–lipid interaction

1. Introduction

The gp120/41 envelope protein is a type 1 integral glycoprotein responsible for the binding and subsequent fusion of HIV-1 to its host cell membrane [1,2]. Upon binding-induced activation, the fusion peptide at the N-terminus of the gp41 transmembrane subunit becomes inserted into the target membrane, thus making gp41 an integral component of two membranes, i.e. virus and target cell [1–3]. Subsequent structural alterations have been postulated to induce apposition of the target cell and viral membranes [4,5]. Previous work seems to indicate that within the fusion loci, apposed target membranes might be distorted by the action of the fusion peptides [6,7]. We show here that the sequence preceding the transmembrane anchor of gp41 may be able to perturb membranes as well.

This Trp-rich sequence, spanning residues 664–683, shows a potential high tendency to partition into the membrane interface as revealed by the interfacial hydrophobicity scale developed by Wimley and White [8–10]. This makes this sequence a suitable candidate to be a membrane-perturbing agent. The high degree of residue conservation and recent mutational analysis highlight the crucial role of this segment in the fusion activity of gp41 [11]. Functional characterization in cells expressing the human immunodeficiency virus type-1 (HIV-1) env mutant products reveals that the pre-transmembrane domain might actually be involved in the opening of the fusion aqueous pore [12].

Using unilamellar vesicles made of an equimolar mixture of dioleoylphosphatidylcholine (DOPC), dioleoylphosphatidylethanolamine (DOPE) and cholesterol (CHOL) as targets we have experimentally demonstrated that a 20 amino acid peptide, corresponding to the region adjacent to the transmembrane segment of gp41, shows a high tendency to partition into membranes. In addition, when in contact with membranes the same peptide can induce liposomal membrane destabilization, i.e. permeabilization, and mixing of bilayer lipids. These effects are promoted by the membrane-associated peptide folded as an α-helix. By contrast a peptide representing a non-functional gp41 as described by Salzwedel et al. [11] was unable to induce lipid mixing in the same lipid system. Moreover, this inactive peptide failed to adopt a helical conformation when associated with membranes. We conclude that the sequence representing a functional gp41 may actually distort membranes and induce the kind of bilayer structural alterations that lead to membrane fusion. Our data are thus consistent with this sequence playing a direct role during the HIV-1 fusion cycle.

2. Materials and methods

DOPC, DOPE, CHOL and the fluorescent probes *N*-(7-nitrobenz-2-oxa-1,3-diazol-4-yl)phosphatidylethanolamine (N-NBD-PE) and *N*-(lissamine rhodamine B sulfonyl)phosphatidylethanolamine (N-Rh-PE) were purchased from Avanti Polar Lipids (Birmingham, AL, USA). 8-Aminonaphthalene-1,3,6-trisulfonic acid sodium salt (ANTS) and *p*-xylenebis(pyridinium)bromide (DPX) were from Molecular Probes (Junction City, OR, USA). *N*-Acetyl-L-tryptophanamide (NATA), octaethyleneglycol monododecyl ether ($C_{12}E_8$) and Triton X-100 were obtained from Sigma (St. Louis, MO, USA). All other reagents were of analytical grade. The sequences NH_2-DKWASLWNWFNITNWLWYIK-COOH (HIV_c) (Fig. 1) and NH_2-DKAASLANAFNITNWLWYIK-COOH (HIV_{c-mut}) were synthe-

*Corresponding author. Fax: (34)-94-4648500.
E-mail: gbpniesj@lg.ehu.es

Abbreviations: ANTS, 8-aminonaphthalene-1,3,6-trisulfonic acid; CHOL, cholesterol; DMSO, dimethylsulfoxide; DOPC, dioleoylphosphatidylcholine; DOPE, dioleoylphosphatidylethanolamine; DPX, *p*-xylenebis(pyridinium)bromide; HIV-1, human immunodeficiency virus type 1; HIV_c, synthetic sequence (20 aa) representing residues 664–683 of HIV-1 gp160 precursor (BH10 viral isolate); LUV, large unilamellar vesicles; NATA, *N*-acetyl-L-tryptophanamide; N-NBD-PE, *N*-(7-nitrobenz-2-oxa-1,3-diazol-4-yl)phosphatidylethanolamine; N-Rh-PE, *N*-(lissamine rhodamine B sulfonyl) phosphatidylethanolamine

0014-5793/00/$20.00
PII: S0014-5793(00)01785-3

sized as C-terminal carboxamides and purified (estimated homogeneity >90%) by Quality Controlled Biochemicals, Inc. (Hopkinton, MA, USA). Peptide stock solutions were prepared in dimethylsulfoxide (DMSO) (spectroscopy grade).

Large unilamellar vesicles (LUV) consisting of DOPC, DOPE and CHOL (molar ratio, 1:1:1), were prepared according to the extrusion method of Hope et al. [13] in 5 mM HEPES, 100 mM NaCl (pH 7.4). Osmolalities were adjusted to 200 mOsm in a cryoscopic osmometer (Osmomat 030, Gonotec, Berlin, Germany). Lipid concentrations of liposome suspensions were determined by phosphate analysis [14]. The average diameter of DOPC/DOPE/CHOL vesicles was of ~130 nm as estimated by quasielastic light scattering using a Malvern Zeta-Sizer instrument.

Partitioning into DOPC/DOPE/CHOL LUV was estimated by physically separating unbound and bound peptide. Unbound peptide was removed from the mixtures by gel filtration in a Sephadex G-75 column. Vesicles labeled with 0.1 mol% N-NBD-PE and N-Rho-PE (1 ml 1 mM total lipid) were incubated at 37°C for 30 min with peptide (0.01 mM) prior to gel filtration. Chromatographed peptide–lipid samples were subsequently solubilized with 2 mM $C_{12}E_8$ in order to minimize the scattering contribution to Trp fluorescence. The Trp and NBD signals allowed simultaneous quantification of co-eluting peptide and lipid respectively.

Membrane lipid mixing was monitored using the resonance energy transfer (RET) assay, described by Struck et al. [15]. The assay, based on the dilution of N-NBD-PE and N-Rh-PE fluorescent probes as lipid mixing is progressing, was adapted to our system as described in [16]. Release of vesicular contents or leakage to the medium was monitored by the ANTS/DPX assay [17]. The procedure is described in detail in [15]. All these fluorescence measurements were conducted in thermostatically controlled cuvettes (37°C) using a Perkin-Elmer LS50-B spectrofluorimeter. The medium in the cuvettes was continuously stirred to allow the rapid mixing of peptide and vesicles.

The analysis of fusion kinetics of DOPC/DOPE/CHOL LUV considered aggregation, dissociation and fusion processes [18,19] and involved the determination of the rate constants of those processes, namely, aggregation C (M^{-1} s^{-1}), dissociation D (s^{-1}) and fusion f (s^{-1}) rate constants. The calculations were performed by introducing certain modifications into the program described in Nir et al. [20].

Infrared spectroscopy measurements were essentially conducted as in [16]. Samples in the absence of vesicles consisted of peptides directly dissolved in D_2O buffer. Before data acquisition these samples were washed four times by centrifugation (peptide fractions were recovered from the pellets). Alternatively, in the presence of vesicles, peptide–lipid complexes were obtained following a flotation protocol (peptide bound to vesicles was recovered from floating fractions) [24]. Infrared spectra were recorded in a Nicolet 550 spectrometer equipped with a DTGS detector. Samples, containing ~4 mg peptide/ml, were placed between two CaF_2 windows separated by 50 μm spacers. 1000 scans (sample) and 1000 scans (reference) were taken for each spectrum, using a shuttle device. Spectra were transferred to a personal computer where solvent subtraction and band position determinations were performed.

3. Results and discussion

Fig. 1A displays the pre-transmembrane gp41 sequence used in this work. The sequence consists of a stretch of uncharged amino acids which is flanked by charged residues. According to the interfacial hydrophobicity scale determined by Wimley and White [8], Trp, Tyr and Phe residues show the highest tendency to partitioning into the bilayer interface. The pre-transmembrane sequence contains one Phe, one Tyr and five Trp residues. This fact explains that the overall interfacial hydrophobicity of the sequence is very high. As shown by the plot depicted in Fig. 1B, three prominent hydrophobic-at-interface regions (main positive peaks above the zero midpoint line) can be discerned within the gp41 subunit. The 'FP' region comprising residues 512–535 [3] corresponds to the fusion peptide. The 'pre-TM' region comprises residues 664–683 and is located immediately preceding the transmembrane anchor. A third region, 'LLP-3', is a leucine zipper-like sequence located within the cytoplasmic tail of the protein, spanning residues 789–815 and representing the lentivirus lytic peptide-3 [21]. The 'FP' and the 'LLP-3' sequences are highly conserved among HIV-1 isolates and have been experimentally shown to interact with and perturb membranes [16,21,22]. Note that the Wimley–White scale is based on different experimental data, and aims at predicting a different property than the commonly used hydropathy scales, so that in fact the former and the latter scales lead to different results when applied to the same peptide [10].

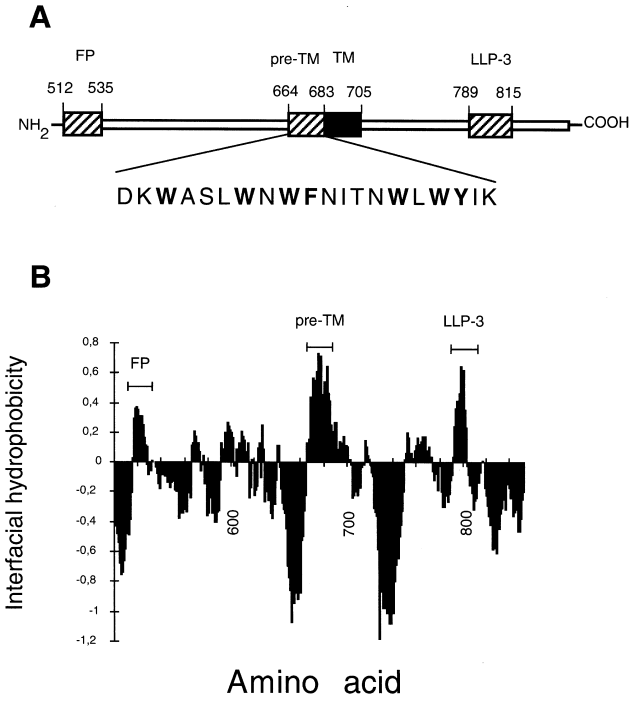

Fig. 1. A: Schematic diagram of HIV-1 gp41 showing the location of hydrophobic-at-interface regions and the pre-transmembrane sequence studied in this work. B: Hydropathy-at-interface plot for HIV-1 gp41. The plotted stretch comprises residues 500–856 of HIV-1 gp160 precursor (BH10 isolate, GenBank M15654). A window of 11 amino acids was used with the hydrophobicity scale at membrane interfaces of Wimley and White [8]. In both panels, designated regions include: FP, fusion peptide; pre-TM, pre-transmembrane segment; TM, transmembrane domain; LLP-3, lentivirus lytic peptide-3.

The above observations prompted us to analyze the 'pre-TM' sequence as a putative membrane-interacting agent. To that end, we made use of a synthetic peptide, HIV_c, representing this region, and model membranes. As target model membranes we selected suspensions of DOPC/DOPE/CHOL unilamellar vesicles. The lipid composition was selected taking into account that the HIV-1 envelope contains high levels of cholesterol and, among phospholipids, phosphatidylcholine and phosphatidylethanolamine are conspicuously represented [23]. The suitability of these vesicles was previously demonstrated in the characterization of the membrane interactions and perturbations caused by the gp41 fusion peptide [24,25]. In addition, they provide a zwitterionic membrane interface analogous to that used by Wimley and White to compose the whole-residue interfacial hydrophobicity scale [8] (Fig. 1).

Trp fluorescence of the peptide incubated in the absence of vesicles decreased with time, intensity becoming stabilized

after ca. 1 h (half-time ca. 15 min) at approximately 30% of the initial value. Upon addition of vesicles, HIV_c Trp emission intensity at 342 nm increased almost instantaneously (data not shown), then decreased, but at a lower rate than when incubated in buffer alone. Since the fluorescence of the soluble Trp analog NATA did not decrease under the same experimental conditions, the intensity decrease in peptide samples was attributed to changes occurring specifically within the HIV_c environment, most likely a self-quenching process arising from peptide aggregation in solution due to its hydrophobic character. Taken together these results suggest that, even if binding to vesicles was much faster, a competing self-aggregation process was decreasing the concentration of unbound monomers in solution.

Consequently, the fraction of peptide monomers available for membrane binding decreased with time. This outcome prevented us from titrating the peptide in solution with increasing amounts of lipid in order to estimate the dissociation constant for the vesicle-bound/free peptide monomer equilibrium.

Therefore, we evaluated binding by physically separating unbound peptide from peptide associated with vesicles by means of gel filtration. Under our experimental conditions

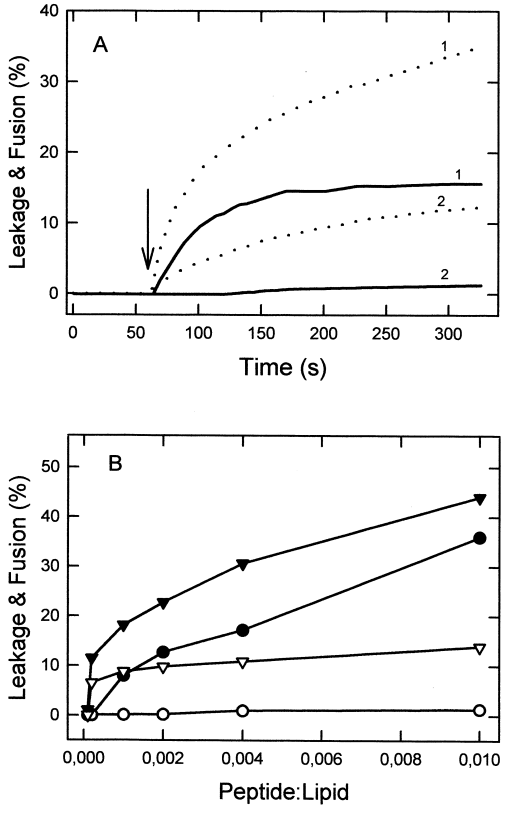

Fig. 2. Peptide-induced destabilization of DOPC/DOPE/CHOL (molar ratio, 1:1:1) LUV as detected by leakage (ANTS/DPX assay) and membrane lipid mixing (RET assay). A: Leakage (dotted lines) and membrane lipid mixing (continuous lines) detected simultaneously as a function of time. HIV_c (1) and HIV_{c-mut} (2) were added (peptide-to-lipid mol ratio, 1:250) to the vesicles (lipid concentration, 50 μM) at the time indicated by the arrow. B: Extents of leakage (inverted triangles) and membrane lipid mixing (circles) as a function of peptide-to-lipid molar ratio (after 5 min.). Filled symbols: HIV_c; open symbols: HIV_{c-mut}. Lipid concentration was 50 μM.

(see Section 2), for a peptide-to-lipid molar ratio of 1:100 we recovered 85–95% of the total amount of HIV_c peptide coeluting with vesicles. Assuming that the number of lipids per HIV_c binding site in the liposomes is comparable to that estimated for fusion peptides of similar size [26], we would obtain an apparent dissociation constant of $\sim$1 μM for the peptide–vesicle binding site equilibrium. Given that the binding process is fast as compared to peptide self-aggregation (see above) we may consider this estimate to be valid to describe the initial partition of the peptide monomers into the DOPC/DOPE/CHOL interface. This would correspond to a local and transient equilibrium. A dissociation constant in the micromolar range under our conditions would indicate that the peptide binds DOPC/DOPE/CHOL vesicles with high affinity.

A high tendency to partition into vesicle membranes was also reflected by the low peptide doses required to destabilize DOPC/DOPE/CHOL LUV (Fig. 2). The HIV_c peptide readily induces leakage of aqueous contents from the vesicles and membrane fusion as evidenced by the occurrence of membrane lipid mixing. Kinetic traces indicated higher initial leakage rates than lipid mixing rates at a fixed peptide-to-lipid molar ratio (Fig. 2A). The extents (after 5 min) of membrane mixing and leakage of contents with increasing amounts of peptide are comparatively shown in Fig. 2B. At an added peptide-to-lipid molar ratio of 1:5000 appreciable leakage could be detected in the absence of lipid mixing. Higher initial rates of leakage and leakage in the absence of lipid mixing seem to indicate that the permeabilization process was not a consequence of leaky fusion induced by the peptide. From these data we can conclude that partitioning of HIV_c into DOPC/DOPE/CHOL vesicles induced two types of destabilization, rupture of the permeability barrier and membrane merging.

In order to judge the functional significance of the membrane perturbations induced by HIV_c, and its specificity as a fusogen, we also measured the ability of HIV_{c-mut} to destabilize vesicles under similar conditions. In the latter sequence the first three Trp residues were replaced by Ala, a substitution known to render a defective gp41 phenotype unable to mediate both cell–cell fusion and virus entry [11]. Results in Fig. 2 clearly indicate that HIV_{c-mut} was also unable to induce significant lipid mixing even at the highest lipid-to-peptide ratio tested of 1:100. The mutant sequence induced partial release of the aqueous contents of the vesicles but always below the levels induced by the functional one. The small leakage caused by HIV_{c-mut} most likely reflects the change in vesicle permeability produced after peptide mass transfer rather than the efflux of aqueous contents through defined pore-like structures.

The results displayed in Fig. 3 prove that the HIV_c peptide behaved as a true fusogen. The kinetics of membrane mixing (curves) are shown together with simulations by means of a mass action kinetic model (dots). The model describes the fusion process as consisting of two steps, aggregation of vesicles, which is a second-order process, and the fusion reaction itself, considered to be a first-order process. The experimental results and calculated values by the model agreed fairly well for HIV_c-induced fusion of DOPC/DOPE/CHOL LUV. This procedure yielded directly the fusion rate constants at different peptide-to-lipid ratios. Changes in this parameter are essential to demonstrate the involvement of a putative fusogen in the fusion reaction itself, as opposed to possible

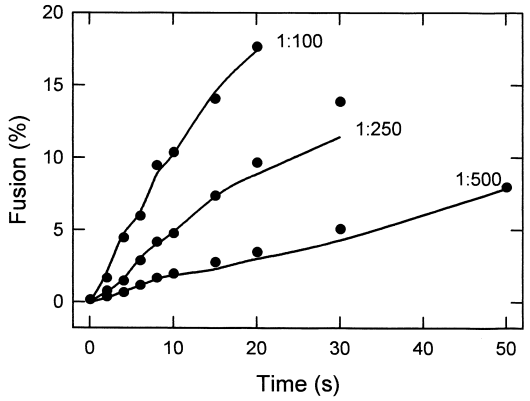

Fig. 3. Kinetics of HIV_c-induced membrane lipid mixing of DOPC/DOPE/CHOL (1:1:1) LUV as a function of peptide-to-lipid molar ratio. Vesicle concentration was 50 μM. Experimental results are given by solid curves. Closed circles indicate values obtained from simulation of the results using a mass action kinetic model (see Materials and Methods).

effects at the level of the preceding aggregation step. Values displayed in Table 1 further demonstrate that, while the aggregation rate constant remained roughly unchanged, the fusion rate constant increased by almost 20-fold from 0.013 s^{-1} to 0.2 s^{-1} when the peptide-to-lipid ratio increased from 1:500 to 1:50 indicating that HIV_c was directly involved in the fusion process. This strongly supports the idea of HIV_c being capable and sufficient for destabilizing two interacting membranes.

Finally, structural infrared spectroscopic results shown in Fig. 4 are consistent with the ability of the HIV_c sequence to fold adopting an α-helix conformation. The amide I band in deuterated buffer (Fig. 4A) shows for HIV_c a maximum appearing at 1644 cm^{-1}. The width of the band precludes the assignment to a single structural component. In the region where the maximum is found, the presence of unordered structures has been described (∼1643 cm^{-1}) together with absorption by α-helical conformations (1641–1658 cm^{-1}) [27]. An additional shoulder at 1574 cm^{-1} comes from side chains of Asp residues. By contrast, within the same amide I region, HIV_{c-mut} predominantly absorbs at 1625 cm^{-1}, a band related to intermolecular interaction of β-like extended conformations. The higher frequency shoulder that appears in the spectrum at ∼1660 cm^{-1} is of uncertain assignment and most likely arises from either parallel β-sheets or β-turns [27].

The spectra in Fig. 4B show again a different conformational behavior of the sequences also in contact with the DOPC/DOPE/CHOL LUV. The spectrum corresponding to HIV_c displays within the amide I region a conspicuous band

Table 1
Rate constants of HIV_c-induced aggregation and fusion of DOPC/DOPE/CHOL LUV[a]

Peptide-to-lipid molar ratio	Rate constant of fusion f (s^{-1})	Rate constant of aggregation C (M^{-1} s^{-1})	Rate constant of dissociation D (s^{-1})
1:50	0.2	8×10^8	0.001
1:100	0.07	8×10^8	0.001
1:250	0.035	5×10^8	0.001
1:500	0.013	5×10^8	0.001

[a]Lipid concentration was constant at 50 μM. Values derived from experiments as shown in Fig. 3.

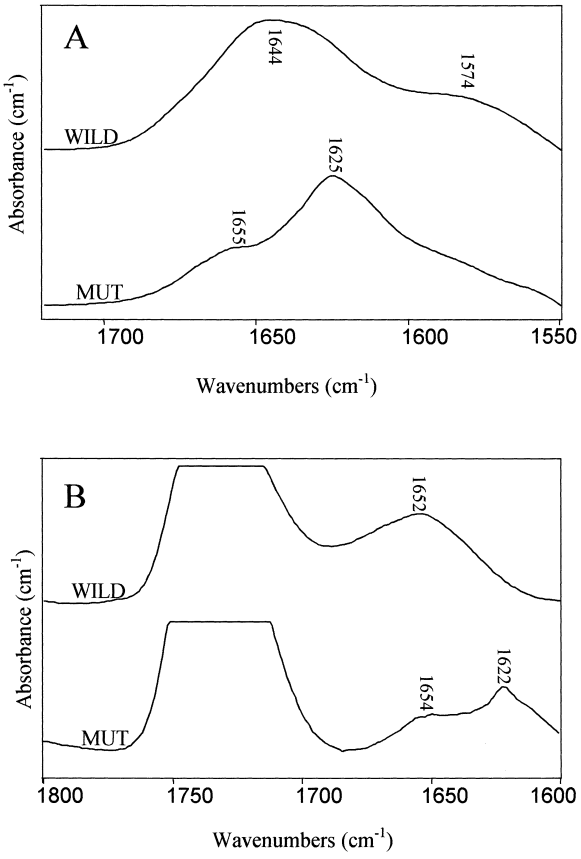

Fig. 4. A: IR spectra of HIV_c (wild) and HIV_{c-mut} (mut) in D_2O buffer. B: IR spectra of HIV_c (wild) and HIV_{c-mut} (mut) associated with DOPC/DOPE/CHOL vesicles. Peptide and vesicles were incubated at a peptide-to-lipid ratio of 1:250, peptide bound to vesicles was subsequently isolated by flotation in D_2O buffer as previously described [16,24].

centered at 1656 cm^{-1} indicative of a preferential α-helical structure adopted by the peptide fraction bound to vesicles. Again the main conformation adopted by HIV_{c-mut} under comparable conditions seems to be different from that of the 'wild-type'. In fact, the presence of lipid bilayers does not appear to modify significantly the conformation of this peptide. Both spectra in Fig. 4B also display a strong absorption at ∼1730 cm^{-1} due to the stretching vibration of phospholipid carbonyl groups. We conclude that the sequence representing the non-functional gp41 is defective in its capacity to fold adopting an α-helical conformation both in buffer and in membranes.

The experimental results in Figs. 1–3 and Table 1, i.e. a tendency to partition into membrane interfaces with high affinity, and an ability to destabilize membranes inducing leakage and fusion, seem to indicate that HIV_c behaves as a membrane-perturbing agent. By comparison HIV_{c-mut}, a peptide representing a defective gp41 pre-transmembrane region, was unable to induce significant lipid mixing and promoted only marginal permeabilization of vesicles. Therefore, these results, together with previous mutational analysis and functional characterization of the mutants in transfected cells [11,12], offer compelling evidence of a direct involvement of the pre-transmembrane gp41 sequence in HIV-1 fusion.

Our structural analysis (Fig. 4) also suggests that adoption of an α-helical conformation by this region might be an im-

portant functional feature of gp41. The possibility that HIV_c in solution might fold partially adopting an α-helical structure indicates that this sequence might have the ability to oligomerize giving rise to assemblies of defined quaternary structure. This feature in turn might be related to the original organization existing in the pre-transmembrane region within the gp41 complex [4,5]. Thus, this sequence might exist as an integral part of gp41 not necessarily in direct contact with the membrane. In such a state, formation of oligomers or interactions with hydrophobic pockets in gp41 might reduce the water accessibility of non-polar surfaces. Nevertheless, our data confirm the intrinsic potential of this sequence to partition into membrane interfaces. It is tempting to speculate at this point that expression of such a potential might be under regulation and evolve only upon fusion activation.

Our results also demonstrate that the membrane-perturbing action of the gp41 pre-transmembrane sequence in the DOPC/DOPE/CHOL system is qualitatively similar to that displayed by the N-terminal fusion peptide [24,25]. Peisajovich et al. [28] have recently reported that the polar region consecutive to the fusion peptide might contribute to its fusogenic activity. Thus, the putative structural organization at the N-terminus of the fusion-active gp41 consisting of a stretch of highly hydrophobic residues inserted into the target membrane, and followed by a fusogenic membrane surface-associated sequence, might be mirrored by sequences in the transmembrane region of the protein ectodomain. In the latter case, insertion through the hydrophobic transmembrane sequence would occur into the virion envelope whereas the adjacent fusogenic sequence would lie associated with the virion membrane interface. Therefore, it is conceivable that both the N-terminal and pre-TM region might be involved in the simultaneous distortion of apposed bilayers at the spots where gp41-mediated fusion is taking place.

Acknowledgements: This work was supported by DGCYT (Grant PB96-0171), the Basque Government (PI 96-46; EX-1998-28; PI-1998-32) and the University of the Basque Country (UPV 042.310-EA085/97; UPV 042.310-G03/98).

References

[1] Moore, J.P., Bradford, A.J., Weiss, R. and Sattentau, Q. (1993) in: Viral Fusion Mechanisms (Bentz, J., Ed.), pp. 233–289, CRC Press, Boca Raton, FL.
[2] Doms, R.W. and Peiper, S.C. (1997) Virology 235, 179–190.
[3] Gallaher, W.R. (1987) Cell 50, 327–328.
[4] Chan, D.C. and Kim, P.S. (1998) Cell 93, 681–684.
[5] Weissenhorn, W., Dessen, A., Harrison, S.C., Skehel, J.J. and Wiley, D.C. (1997) Nature 387, 426–428.
[6] Colotto, A. and Epand, R.M. (1997) Biochemistry 36, 7644–7651.
[7] Pereira, F.B., Valpuesta, J.M., Basañez, G., Goñi, F.M. and Nieva, J.L. (1999) Chem. Phys. Lipids 103, 11–20.
[8] Wimley, W.C. and White, S.H. (1996) Nature Struct. Biol. 3, 842–848.
[9] White, S.H. and Wimley, W.C. (1999) Annu. Rev. Biophys. Biomol. Struct. 28, 319–365.
[10] Suárez, T., Gallaher, W.R., Agirre, A., Goñi, F.M. and Nieva, J.L. (2000) J. Virol. in press.
[11] Salzwedel, K., West, J. and Hunter, E. (1999) J. Virol. 73, 2469–2480.
[12] Muñoz-Barroso, I., Salzwedel, K., Hunter, E. and Blumenthal, R. (1999) J. Virol. 73, 6089–6092.
[13] Hope, M.J., Bally, M.B., Webb, G. and Cullis, P.R. (1985) Biochim. Biophys. Acta 812, 55–65.
[14] Böttcher, C.S.F., van Gent, C.M. and Fries, C. (1961) Anal. Chim. Acta 24, 203–204.
[15] Struck, D.K., Hoekstra, D. and Pagano, R.E. (1981) Biochemistry 20, 4093–4099.
[16] Nieva, J.L., Nir, S., Muga, A., Goñi, F.M. and Wilschut, J. (1994) Biochemistry 33, 3201–3209.
[17] Ellens, H., Bentz, J. and Szoka, F.C. (1985) Biochemistry 24, 3099–3106.
[18] Nir, S., Bentz, J., Wilschut, J. and Düzgünes, N. (1983) Prog. Surf. Sci. 13, 1–124.
[19] Bentz, J., Nir, S. and Wilschut, J. (1983) Colloids Surf. 6, 333–363.
[20] Nir, S., Stegmann, T. and Wilschut, J. (1986) Biochemistry 25, 257–266.
[21] Kliger, Y. and Shai, Y. (1997) Biochemistry 36, 5157–5169.
[22] Rafalski, M., Lear, J. and DeGrado, W. (1990) Biochemistry 29, 7917–7922.
[23] Aloia, R.C., Tian, H.R. and Jensen, F.C. (1993) Proc. Natl. Acad. Sci. USA 90, 5181–5185.
[24] Pereira, F.B., Goñi, F.M., Muga, A. and Nieva, J.L. (1997) Biophys. J. 73, 1977–1986.
[25] Nieva, J.L., Nir, S. and Wilschut, J. (1998) J. Liposome Res. 8, 165–182.
[26] Rafalsky, M., Ortiz, A., Rockwell, A., van Ginkel, L., Lear, J.D., DeGrado, W. and Wilschut, J. (1991) Biochemistry 30, 10211–10220.
[27] Arrondo, J.L.R. and Goñi, F.M. (1999) Prog. Biophys. Mol. Biol. 72, 367–405.
[28] Peisajovich, S.G., Epand, R.F., Pritsker, M., Shai, Y. and Epand, R.M. (2000) Biochemistry 39, 1826–1833.